A STUDY OF PROPELLER-WING-BODY INTERFERENCE FOR A LOW SPEED TWIN-ENGINED PUSHER CONFIGURATION

Michael George Maunsell*
Universidade de São Paulo, Brazil

Abstract

This paper presents the results of an experimental and theoretical study of a twin-engined pusher wing-fuselage configuration suitable for general aviation.

The experimental investigation was based on wind tunnel tests using a half wing-body model and nine different propeller positions.

Two basic flow conditions were explored:

(i) A high speed cruise, low propeller thrust with J=0.74 C =0.017

(ii) A low speed flight, high propeller thrust with J=0.14 c =0.095

Results include thrust grading curves across the vertical and horizotal radii of the propeller disc and chordwise static pressure plots at four spanwise stations on the inboard wing.

A theoretical study was made using an existing panel programme combined with the linear theory of propeller-wing-body interaction of Koning .

Comparison showed reasonable agreement between experimental and theoretical results, including those for the high thrust case which was expected to lay outside the normally accepted range of propeller velocity ratios predictable by linear theory.

Conclusions are made with respect to the propeller positions used and to their application with regard to design projects in two basic categories of performance of short range STOL and long range cruise .

Nomenclature

c	=chord of a wing section
$\bar{c}$	=mean chord of the wing
$\bar{C}_D$	=drag coefficient of the wing only=D/qS
$\bar{C}_L$	=lift coefficient of the wing only=L/qS
C_L	=lift coefficient of a section of the wing=L/qc
$\bar{C}_M$	=pitching moment coefficient of the wing about the quarter chord line=m/qS
C_p	=pressure coefficient=(p -p)/q
C_T	=propeller thrust coefficient= n D
D	=propeller disc diameter
$D.dC_T/dr$	=thrust grading value at some point on the propeller blade
J	=propeller advance ratio=V/nD
L	=lift on the wing or on a section of the wing
m	=pitching moment acting about the quarter chord line of the wing
$\bar{n}_p$	=the unit vector normal to the surface at the point P
N_μ	=the total number of discrete vortex panels in the configuration
N_σ	=the total number of source panels on the surface of the configuration
p	=local static pressure
p_o	=static pressure in the freestream
q	=freestream dynamic pressure
r	=local radius
R	=propeller tip radius
S	=wing area
T	=propeller thrust
$\bar{V}_\infty$	=freestream velocity
$\bar{V}_p$	=velocity at the point P
$\bar{V}_{pp}$	=induced velocity at the point P due to the propeller or propellers
$\bar{V}_\mu$	=induced velocity at the point p due to vortex panels
$\bar{V}_\sigma$	=induced velocity at the point P due to the source panels
x	=distance downstream of the wing leading edge
α_c	=angle of incidence of wing, corrected for wind tunnel interference
γ	=local vorticity
ρ	=air density
σ_p	=distributed source intensity on the panel at point P

* Lecturer, Laboratorio de Aeronaves, Departamento de Engenharia Mecanica, Escola de Engenharia de Sao Carlos, U.S.P., Av. Dr. Carlos Botelho, 1465 13560 - S.Carlos - S.P., Brazil.

Introduction

Investigations into propeller-wing-body interaction date back to the early days of aviation. Some of the first research was published by Fage and Howard[1] in Britain and Warner[2] at NACA in the United States closely followed by Prandtl[3] in Germany. During the following period the main emphasis was placed on experimental work on both sides of the Atlantic, with the volume of work of Lock et al[4,5,6,7] following Fage's work, published as Aeronautical Research Council R&Ms and later that of Wood et al[8,9,10,11,12,13] at NACA outstanding.

The above mentioned work yielded a large volume of data suitable for aircraft design requirements of the time. However the nacelle and wing

geometries of that period tended toward rather high parasite drag and large regions of seperated flow which severely limit the use of the information in the design of modern aircraft. Lock[5,14] also developed analytical theory on the intereference between a propeller and the body close downstream. However, in 1935 Koning[15] presented what may still be considered as one of the most thorough analyses of propeller-wing-body interference, based on actuator disc theory and including the effects of the propeller when mounted upstream or downstream of the wing. His work is naturally limited to analytical theory and, with respect to downstream effects, has been made obselete by more modern numerical methods.

in 1959 Ribner[16] introduced a more exact theory which included the trailing vorticity within the slipstream downstream of the propeller. Ellis[17,18] later successfully modified Ribner's theory and proposed a numerical procedure which overcame the limitations on the aspect ratio of the downstream wing segment directly influenced by the slipstream.

Rethorst[19] in 1958 had presented a similar solution to that proposed by Ribner which was analytical rather than numerical and therefore more restricted in its general application.

Much further experimental and theoretical work has been done on the problem of downstream wing-slipstream interaction up to the present, however the author has not found any further reference to the problem treated in this work, of the interaction of a downstream propeller on the rest of the aircraft upstream of its position.

In 1984 the current state of the art was given in the proceedings of the AGARD Fluid Dynamics Symposium[20] in Toronto at which an oral presentation summarising the present work was made.

The work presented here refers specifically to the pusher propeller layout and the experimental results were aimed at providing a relatively wide data base, giving experimental results for both the propeller and the upstream wing for each case, for eventual use in the comparison of theoretical results.

Experimental Details

The experimental model consisted of a 1.5m span half-model wing and fuselage which was mounted on one wall of the Southampton University 1.68m x 2.13m low speed wind tunnel. A three-bladed 0.5m diameter model propeller, driven by a 4 pole variable frequency electric motor giving approximately 5HP at 5000 rpm was mounted seperately.

The wing,which used a NASA GA(W)-1 aerofoil section was attached to the balance lift struts, while the semi-fuselage was fixed solidly to the wind tunnel wall. The wing was slotted into the fuselage a distance of 7.5cms with an 8mm gap around the wing at the root. The gap was sealed for pressure measurements and left open for balance measurements.

Transition strips were attached to the fuselage and wing but the wooden model propeller blades were left free.

The nine propeller positions and four chordwise sections of the wing at which pressure plots were made are shown in Figure 1, (see A,B,C and D, and P1 to P5 and I,II,II and IV respectively). The propeller axis was maintained parallel to the fuselage and the tunnel centreline and the direction of rotation of the propeller was clockwise when observed from the rear facing forwards.

Two basic aerodynamic conditions were applied of J=0.74 and C =0.17 and J=0.14 and C =0.095 giving model Reynolds Numbers of 1,64x10 and 6.15x10 respectively.

Propeller thrust grading was measured using the technique pioneered by Fage[21] of measuring the

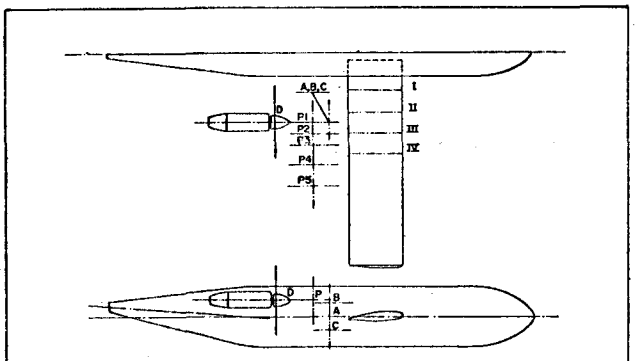

FIG. 1- GENERAL LAYOUT OF THE EXPERIMENTAL HALF-MODEL

thrust grading along the propeller blade by use of a total head rake mounted close to the downstream side of the propeller. Horizontal and vertical total head rake positions H1,H2,V1 and V2 are shown in Figure 2.

Experimental Results

Propeller thrust grading curves of D.dC /dr against r/R are shown in Figure 2 for propeller positions A,B and C under low power conditions, (i.e. low thrust, high speed cruise).

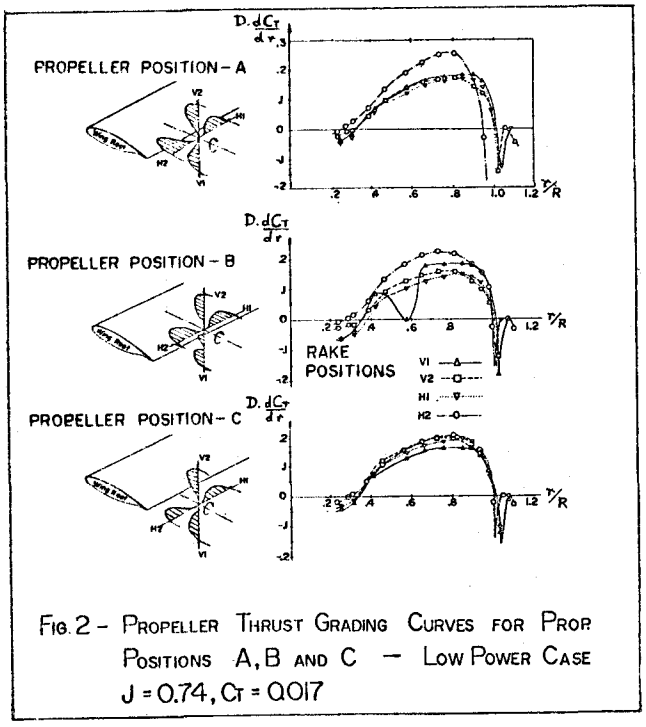

FIG. 2 - PROPELLER THRUST GRADING CURVES FOR PROP POSITIONS A, B AND C - LOW POWER CASE J = 0.74, C_T = 0.017

The effect of the local airflow on the propeller thrust grading may be considered as a combination of two effects:

(i) that due to the generally non-axial direction of the inflow to the propeller.

(ii) that due to the local effect of the wing wake striking the propeller.

Figure 2 shows the first effect to be most pronounced in the central position A in which the hub of the propeller is directly downstream of the wing trailing edge and position B when the hub is aligned above the trailing edge. A general increase in thrust grading values along the radius H2 is due to the combination of the direction of propeller rotation and the downwash behind the wing, giving a local high angle of attack to the blade. radii V2 and H1 are of lower thrust and very similar one to the other.

The second effect is shown at radius V1 for propeller positions B and C as a local drop in thrust grading values at the intersection of the wing wake with the propeller blade along that radius.

Figure 3 shows much the same general layout to the thrust grading curves, with the same sequence of H2,V2,H1,V1 for highest to lowest thrust values respectively, with effect (ii) at radius V1 varying according to the state of the wing wake at the intersection with the propeller.

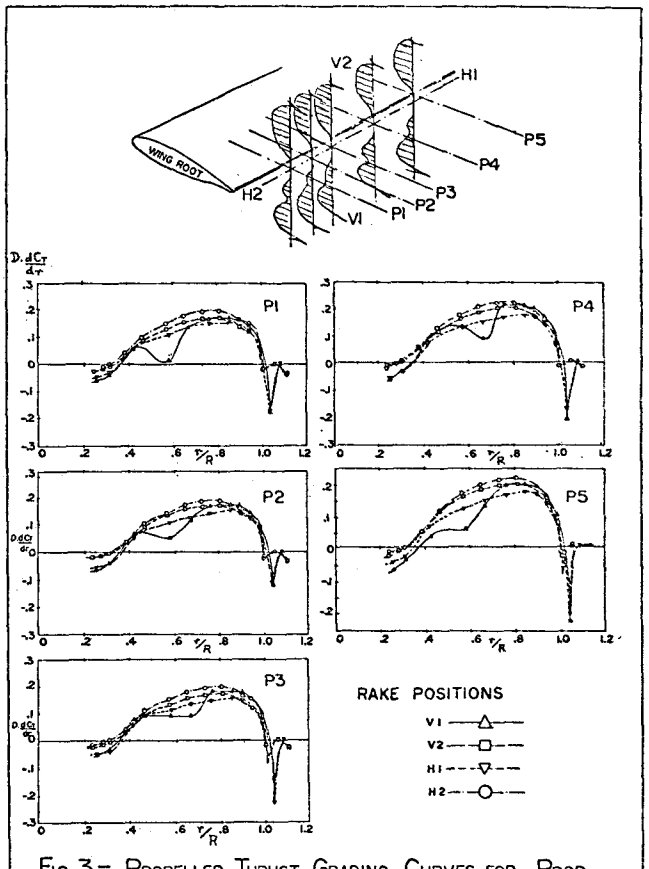

FIG. 3 - PROPELLER THRUST GRADING CURVES FOR PROP POSITIONS P1 TO P5 - LOW POWER CASE
J = 0.74, C_T = 0.017

It is noticeable that both effects (i) and (ii) are more pronounced at low thrust and high speed than at high thrust and low speed. Local variations in propeller inflow velocity represent a larger proportion of the total velocity over the propeller blade at low power and a rotation of 3800 rpm, as compared to the high power case with 5000 rpm propeller rotation.

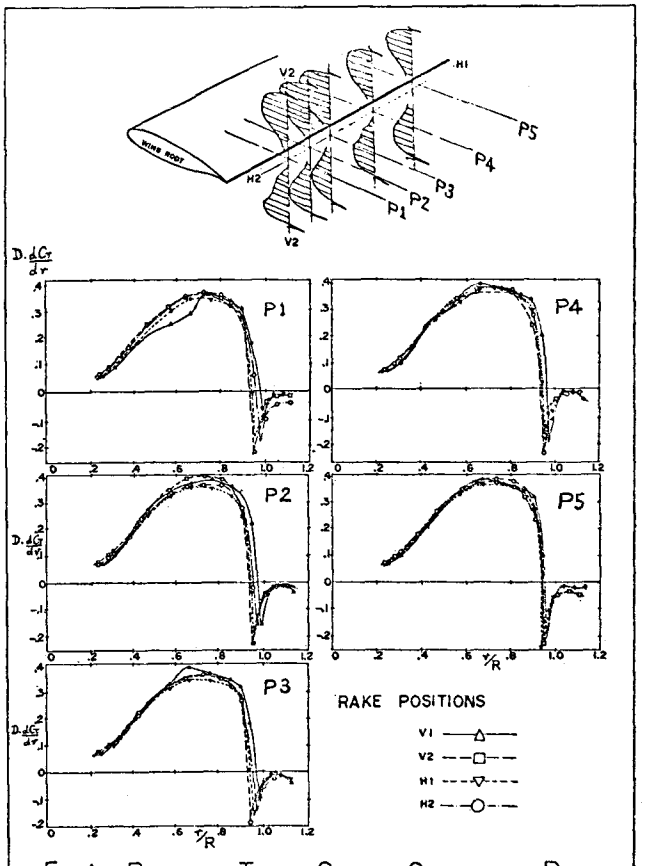

FIG. 4 - PROPELLER THRUST GRADING CURVES FOR PROP POSITIONS P1 TO P5 - HIGH POWER CASE
J = 0.14, C_T = 0.095

In the high power case, shown in Figure 4, propeller effect (i) is very small when compared to that registered for the low power case and even the overall influence of effect (ii) on total thrust, (the area under the curve), is greatly decreased. The curves for propeller positions P1 to P5 are shown only, as those for positions A,B and C showed virtually no difference to that of position P5, that is, the thrust grading distribution for all four propeller radii were so closely grouped as to be indistinguishable. In this respect, it is interesting to compare the curves of Figure 4 with the high power curve in the lower righthand corner of figure 5, which shows the almost negligible influence of effect (i) under the high power conditions presented here.

Effect (ii) is significant only for the most inboard propeller position.

Figure 5 compares the thrust grading curves with the greatest variations in radial distributions, for both low power and high power cases, compared to the results obtained for the propeller alone in the wind tunnel.

The results for propeller position D at both low and high power differed insignificantly from those for the propeller alone in Figure 5 and are not included.

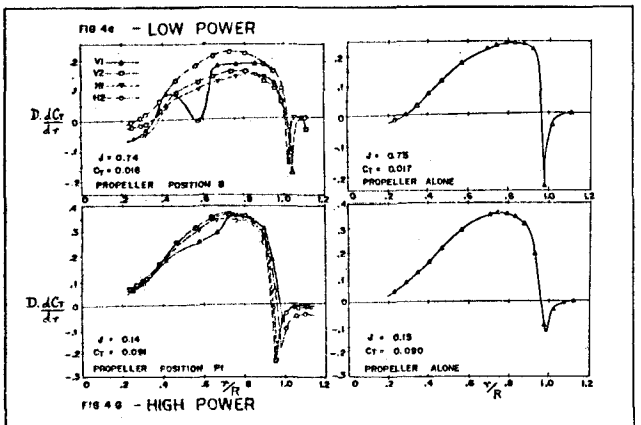

Fig 5 - Comparison of Typical Propeller Thrust Grading Curves.

Experimental Chordwise Pressure Distribution

The chordwise pressure distributions C_p against x/c for wing sections I,II,III and IV for propeller position A at low power are shown in Figure 6 and compared with those for propeller positions A,B and C at high power.

The results for all propeller positions at low power as presented in Figure 6 were shown to be very similar to those for the power off condition, the result for propeller position A is shown here as a typical example for comparison with the high power results.

The effect of the propeller at high power is evident in the form of generally lower values of C_p on both upper and lower surfaces. Propeller position B shows the most pronounced increase in lift associated with a low pressure plateau over the rear part of the wing upper surface at sections II and III.

Figure 7 shows the experimental chordwise distribution for propeller positions D and P1,P2 and P3. The latter are included here as of interest with respect to the more conventional inboard propeller positions. The lessening of the propeller suction effect over the rear upper surface with the change in propeller position is evident, as is the decrease in pressure difference between upper and lower wing surfaces near the trailing edge for the most distant propeller position D.

Results for propeller positions P4 and P5 are available, but are not included here.

Tables of Wing Only Aerodynamic Coefficients

The wind tunnel measurements of lift, drag and pitching moment, upon which the overall values of $\bar{C}_L/\bar{C}_D$ and $\bar{C}_M$ for the model are based, were measured for the wing only since the fuselage was fixed rigidly to the tunnel wall, as explained above. (The bar over the parameters indicates reference to the complete wing rather than to a particular wing section).

The experimental lift/drag ratios for the low power condition shown in Table 1 are lower than might be expected for a wind tunnel investigation. However the Reynolds number of the tests was small and the experimental aerofoil possessed a stowed 30% chord full-span Fowler flap, shown in Figure 8, which modified the trailing-edge area of the GA(W)-1 aerofoil increasing the drag. The experimental

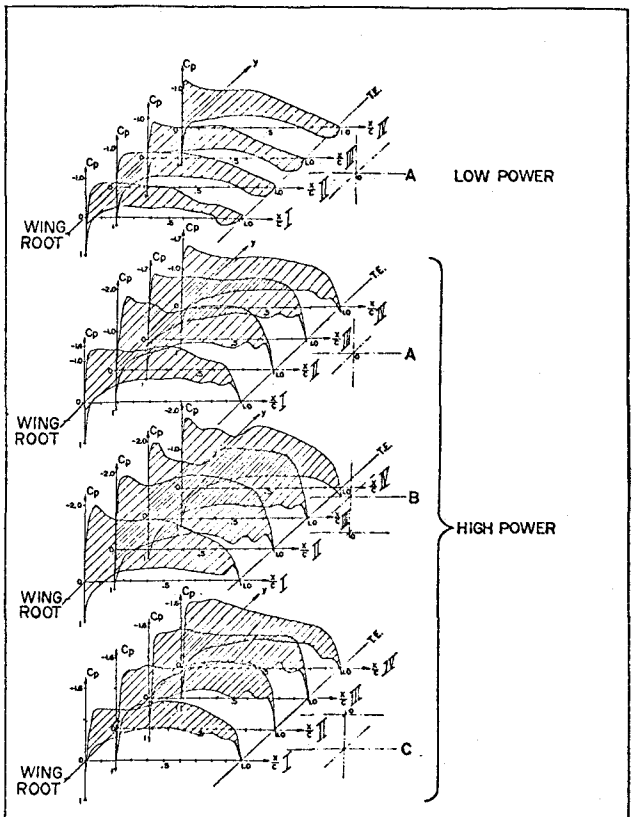

Fig 6 Pressure Distributions over Inboard Wing

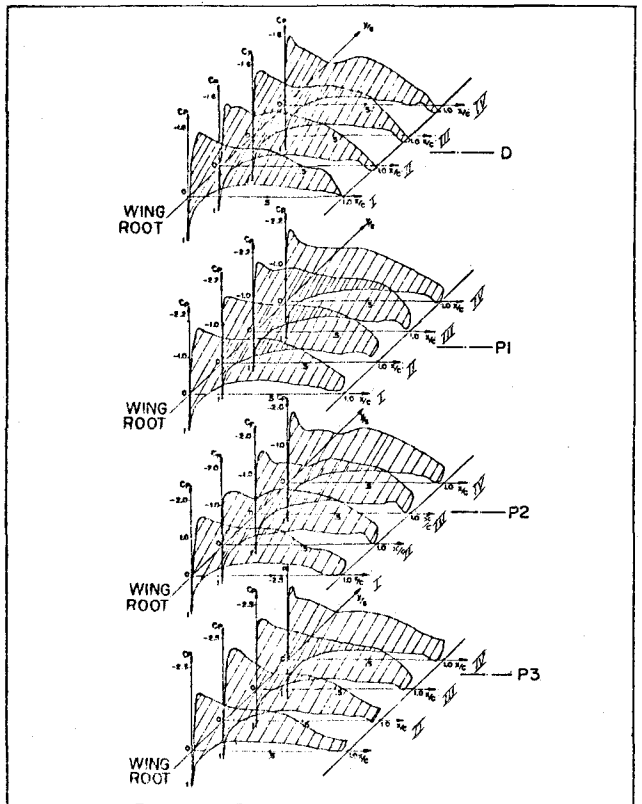

Fig 7 — Pressure Distributions over Inboard Wing
High Power Case — J = 0.14 C_T = 0.095

lift/drag ratio of the wing with no propeller was $\bar{C}_L/\bar{C}_D$= 22.9, which is shown to be significantly diminished by the propeller interaction. The chordwise pressure distributions for low power showed a difference in C_p of the order of -0.1 at the trailing edge of the wing, an example of which is shown in Figure 8 for propeller position A. This indicates an increase in pressure drag due to the low pressure induced by the propeller on the flat vertical face at the rear of the GA(W)-1 aerofoil.

Table 1. Experimental Values of $\bar{C}_L/\bar{C}_D$, C_M and C_{Mp} at Low power

Propeller Positions	$\bar{C}_L/\bar{C}_D$	$\bar{C}_M$	$\bar{C}_{Mp}$	NOTES
A	11.6	-.084	0	
B	11.5	-.087	-.008	
C	14.8	-.089	+.008	ΔC_{Mp} is the increase in C_M due only to propeller thrust calculated from transducer measurements at the motor supports within the nacelle.
D	13.2	-.087	-.010	
P1	14.2	-.086	-.008	
P2	14.8	-.086	-.008	
P3	14.1	-.086	-.008	
P4	13.3	-.084	-.008	
P5	12.7	-.086	-.008	

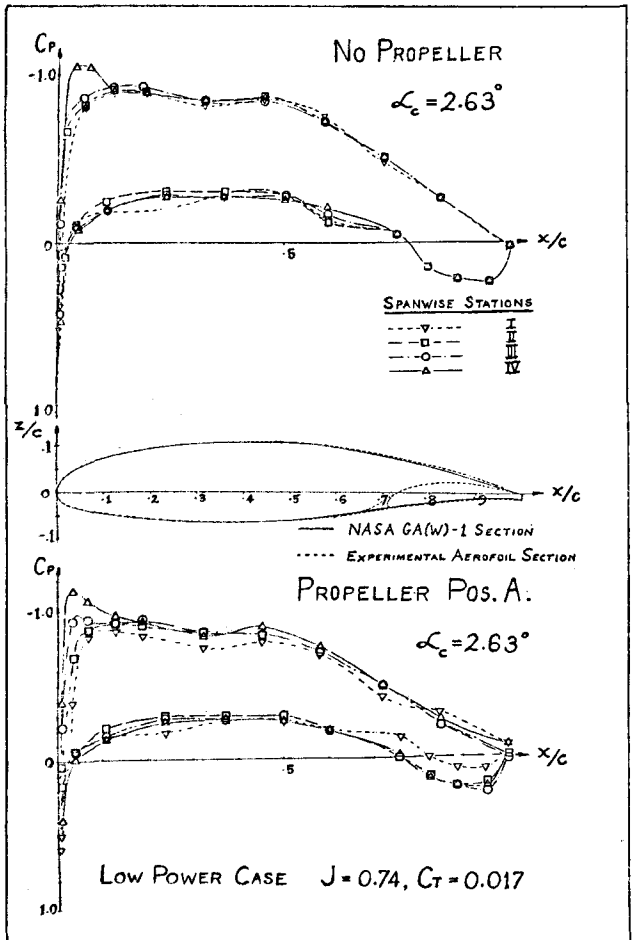

Fig. 8 - Aerofoil Shape and Pressure Distribution

The inboard propeller positions A and B, directly behind and above the trailing edge, and the most outboard position P5 are those which most adversely affect the cruise performance of the configuration. The values of $\bar{C}_M$ for the wing with the propeller at low power differ marginally from the no-propeller case of $\bar{C}_{M_o}$=-081. The effect of the propeller is shown to be an increase in the negative moment of the the order of 10% of $\bar{C}_{M_o}$.

Hence, in the cruise case, the propeller inflow does not adversely affect the pitching moment of the wing to a great degree in all propeller positions, whereas, as noted above, there is an adverse effect on the drag of the wing.

Values of lift and and pitching moment coefficents for the high power condition are shown in Table 2 and $\Delta\bar{C}_L$ and $\Delta\bar{C}_M$ refer to the difference between these values and those for no propeller, that is, they refer directly to the propeller effect. The high values of these latter for propeller position B and less so for positions P1 and P2 reflect the chordwise pressure distributions shown in Figures 6 and 7.

Table 2. Experimental Values of $\bar{C}_L$, $\Delta\bar{C}_L$, $\bar{C}_M$ and $\Delta\bar{C}_M$ at High Power

Propeller Position	$\bar{C}_L$ Experimental	$\Delta\bar{C}_L$ Experimental	$\bar{C}_M$ Experimental	$\Delta\bar{C}_M$ Experimental
A	0.772	0.222	- 0.125	- 0.044
B	1.025	0.475	- 0.165	- 0.084
C	0.552	0.002	- 0.103	- 0.022
D	0.701	0.151	- 0.103	- 0.022
P1	0.859	0.309	- 0.145	- 0.064
P2	0.883	0.333	- 0.145	- 0.064
P3	0.843	0.293	- 0.124	- 0.043
P4	0.867	0.317	- 0.145	- 0.064
P5	0.788	0.238	- 0.124	- 0.043

Spanwise Lift Distribution

Experimental and theoretical results are compared in Figure 8.

A simple schematic diagram is included for each propeller position showing a portion of the fuselage section, at the origin of the coordinates C_p and y/s and the relative position of the propeller. The interference effects of the propeller on the wing at low power are very small and all nine propeller positions yielded very similar results to those shown here for position P2.

The results for high power show disagreement between the potential theory and experimental measurements in the root area for propeller

positions close to the root. Boundary layer interaction with the propeller flow field is likely to be accentuated in this area causing the loss of lift shown here when compared to the results of potential theory.

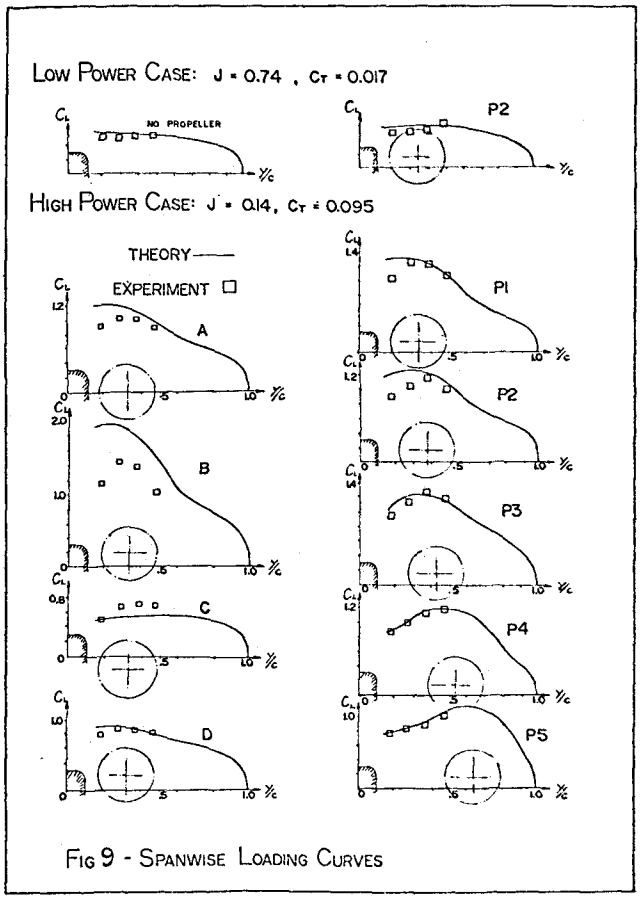

FIG 9 - SPANWISE LOADING CURVES

The Theoretical Method

The theoretical method was based on a potential flow panel program developed by Butter[22,23] from an original MBB first order panel method. The method used constant source distributions over each external panel and descrete vortices over the wing camber and wake surface.

The unknown parameters were the source distributions on the external panels and the circulation at wing spanwise stations defined by each chordwise strip of wing panels, while the chordwise vortex distribution was predetermined.

Butter showed that the best results using the original panel programme were obtained by applying the Birnbaum flat plate solution to the chordwise vortex distribution, in which

$$Y \propto \left(\frac{1-x}{x}\right)^{\frac{1}{2}}$$

The values of the unknowns were obtained in the usual way by applying the Neumann condition of zero normal velocity to each surface panel and the Kutta condition at the trailing edge of each spanwise station mentioned above.

The normal velocity component due to each propeller at each panel collocation point was calculated using the linear theory of Koning and added to that due to the freestream, as shown in the equation below. These were then added to the normal velocity components due to the source and vortex distribution described above. The final component is that due to the source distribution of the panel on which the collocation point P is located. If the collocation point is on a vortex panel, in the case of a Kutta Point, then all N source panels are included in the summation of the third component and the final component on the lefthand side vanishes.

The total velocity normal to a source panel is thus shown in the following expression,

$$\left(\bar{V}_\infty + \bar{V}_{pp}\right)_p + \frac{1}{4n}\left(\sum_{1}^{N_\sigma - 1} \bar{V}_{p\sigma} \cdot \bar{n}_p + \sum_{1}^{N_\mu} \bar{V}_{p\mu} \cdot \bar{n}_p\right) + \frac{1}{2}\sigma_p = \bar{V}P \cdot \bar{n}_p$$

The values thus obtained were then substituted in the expression below for the velocity tangential to each panel surface, which, of course again includes the effect of the propellers.

$$\bar{V}_p = \bar{V}_\infty + \bar{V}_{pp} + \frac{1}{4n}\left(\sum_{1}^{N_\sigma - 1} \bar{V}_{p\sigma} + \sum_{1}^{N_\mu} \bar{V}_{p\mu}\right) + \frac{1}{2}\sigma_p \bar{n}_p$$

The theoretical results include values of J well outside those normally permitted in linear theory. However, Koning pointed out that for the wing upstream of the propeller the effect of the vorticity in the wake downstream of the propeller may be neglected, thus this non-linear component of the propeller interference on the wing was ignored, allowing linear theory to be applied to both the low and high power cases.

A relatively primitive model of the propeller slipstream was used in this study and it is felt that the use of a more complex modelling technique would undoubtedly improve the results. Further work is continuing in this area.

Conclusions

a) It was found that the effect of wing-body interference on the propeller was much greater in the low power (cruise) case than in the high power case, both in terms of the resultant general non-uniform thrust distribution over the propeller disc and in the local effect of the wing wake striking the propeller. These latter effects were most pronounced in the mid and upper inboard propeller positions A and B.

b) Experimental results for both low and high power cases showed differences near the wing root from theoretical predictions. The differences are probably due to propeller induced effects combined with the effects of the boundary layer near the wing root junction.

c) Propeller interaction with the wing at high thrust and low freestream velocity show that wing lift is markedly increased by the propeller influencee for all propeller positions except the lower inboard position C close to and below the

wing trailing edge. In this position the propeller has negligible effect on lift.

d) The general trends shown by the experimental results of lift distribution over the wing at high power, confirmed by the theory, suggest that the the theory may have a wider application than was predicted. A tentative conclusion is that the incorporation of Koning's theory into this panel method is suitable for a preliminary study of propeller-wing interaction for a pusher layout over the whole flight envelope.

e) All experimental propeller positions showed an increase in negative pitching moment of the wing over that of the wing without the propeller due to the interference of the propeller in the form of suction over the rear surfaces of the wing.

An overall study of the experimental results reveals certain conclusions as to the advantages and disadvantages of each propeller position with respect to their use in design projects, here divided for simplicity into two categories:

Short Range STOL Performance:

Propeller position B shows the highest increase in lift due to the propeller influence at high thrust and low speed, however this position is also located close to the fuselage and would thus undoubtedly suffer from the effects of structural vibration and propeller noise within the cabin.

The prefered option would be propeller position P2 which offers slightly less lift at high power and greater assymetry in a one-engine-off situation. This position also gives the best lift/drag ratio in the low power (cruise) condition.

Long Range Cruise Performance:

As shown above, position P2 gives the highest lift/drag ratio. Position C shows the same value for lift/drag, however it gives no change in lift at high power.

A further option, which does not have the limitations of the positions mentioned above, is the rear inboard position D which shows moderate values of lift/drag at low power and high speed and propeller induced lift at high power and low speed, while one-engine-off asymmetry is minimized.

Further Work

The theoretical programme in its present form showed promise as a method of assessment of the aerodynamic characteristics of a multi-engined pusher propeller wing-body configuration and particularly in the design mode to find suitable propeller positions for a given layout.

A potential exists for much further theoretical work in the area including viscous effects and the use of a more complex geometrical model in the panel analysis and work is under way on a more exact representation of the propeller slipstream for the pusher propeller based on the method of Shollenberger[24].

A theoretical analysis of the interference effects of the wing-fuselage on the propeller in the downstream position and the development of a more complex model of the propeller slipstream as a result of this interaction is also envisaged.

With regard to the experimental work, a further aspect of the general problem that might be investigated is that of the influence of the direction of rotation of the propeller, particularly in relation to non-uniform disc loading at low thrust and high speed, as shown above for propeller positions A and B in Figure 2.

Summing up with respect to the present work, we can say that the experimental data bank used in conjunction with the theoretical programme provides a reasonable general basis for the analysis of propeller-wing-body interaction with regard to the use of propellers downstream of the wing.

References

[1]Fage,A.and Howard,R.G.,"On the Modification of the Performance of an Airscrew due to the propinquity of a Plane Surface: also Experiments with the same Model Airscrew when mounted behind a Model of a Power Car of Airship R.32,"A.R.C.R&M No.682, 1920.

[2]Warner,E.P.,"Slipstream corrections in Performance Computation",NACA Rep.71,1920.

[3]Prandtl,L.,"Mutual Influence of Wings and Propellers",NACA TN74,Dec.1921.

[4]Lock,C.N.H.and Bateman.H.,"The Measurement of Airflow around an Airscrew",A.R.C.R&M No. 955 Vol.II,1924-1925

[5]Lock,C.N.H.,Bateman.H.and Townend,H.C.H.,"The Airflow around a Body as affecting Airscrew Performance",A.R.C.R&M No.956,1925.

[6]Lock,C.N.H. and Bateman,H., "Analysis of Experiments on the Interference between Bodies and Tractor and Pusher Airscrews",A.R.C.R&M No.1445,1931

[7]Lock,C.N.H. and Bateman,H., "Interference between Bodies and Airscrews, Parts I and II", A.R.C.R&M No.1522,1932.

[8]Wood,D.H., "Tests of Propeller Nacelle Combinations in Various Positions with reference to the Wings. Part I - Thick Wing-NACA Cowled Nacelle Tractor Propeller",NACA TR415,1932.

[9]Wood,D.H.,Idem, "Part II - Thick Wing-Various Radial Cowlings-Tractor propeller",NACA TR436,1932.

[10]Wood,D.H.,Idem,"Part III - Thick Wing-Various Radial Cowlings-Pusher Propeller",NACA TR462,1933.

[11]Wood,D.H.,Idem,"Part IV -Biplane- Radial Engine Cowlings-Pusher Propeller",NACA TR506,1934.

[12]Wood,D.H.and Bioletti,C., "Tests of Propeller Nacelle Combinations in Various Positions with reference to the Wings. Part VI-Wings and Nacelles with Pusher Propeller",NACA TR507,1934.

[13]Wood,D.H.,"Engine Nacelles and Propellers and Airplane Performance",SAE Journal, p.148-160, April 1936.

[14]Lock,C.N.H., "Theory of Airscrew Body Interference, Applications to Experiments on a Body of Fineness Ratio 3.0 with Tractor Airscrew", A.R.C.R&M No.1378,1930.

[15]Koning,C."Influence of the Propelller on Other Parts of the Airplane Structure", Division M, Aerodynamic Theory, Vol.IV, edited by Durand,W.F., C.I.T. California,1935.

[16]Ribner,H.S.,"Theory of Wings and Slipstream", University of Toronto, UTIAS Report 60, Inst.of Aerophysics,1959.

[17]Ellis,N.D.,"A Computer Study of a Wing in a Slipstream",UTIAS Technical Note No.101,feb.1967.

[18]Ellis,N.D., "Aerodynamics of Wing-Slipstream Interaction:A Numerical Study",UTIAS Report No.169, Oct.1971.

[19]Rethorst,S."Aerodynamics of Nonuniform Flows as Related to an Aerofoil Extending Through a Circular Jet", Jour.of the Aero.Scs.,Jan.1958.

[20]AGARD Conference Proceeedings No.366 - "Aerodynamics and Acoustics of Propellers",Fluid Dynamics Symposium, Toronto, Canada,1-4 October 1984.

[21]Fage,A.,"a Note on the Method of Estimating from Observations of Total Head, the Total Thrust of an Airscrew",A.R.C.R&M No.699,Oct. 1920

[22]Butter,D.J.,"Program Specification for the MBB Panel Method",Hawker Siddeley Aviation Ltd.Report No.HSA-MAE-R-CMP-0007,July 1977.

[23]Butter,D.J., "Improvements to the Basic MBB Panel Method",Hawker Siddeley Aviation Ltd.Report No.HSA-MAE-R-FDM-0006,Feb.1977.

[24]Shollenberger,C.A.,"Three-Dimensional Wing/Jet Interaction Analysis Including Jet Distortion Influences",AIAA Paper 73-655,Palm Springs, California, 1973.